Wind and Structures, Vol. 14, No. 6 (2011) 559-582
DOI: http://dx.doi.org/10.12989/was.2011.14.6.559

Occupant comfort evaluation and wind-induced serviceability design optimization of tall buildings

M.F. Huang[1,2], C.M. Chan*[2] and Kenny. C.S. Kwok[3]

[1]*Institute of Structural Engineering, Zhejiang University, Hangzhou 310058, P.R.China*
[2]*Department of Civil and Environmental Engineering, Hong Kong University of Science and Technology, Hong Kong*
[3]*School of Engineering, University of Western Sydney, NSW, Australia*

(Received July 8, 2010, Revised February 14, 2011, Accepted April 7, 2011)

Abstract. This paper presents an integrated wind-induced dynamic analysis and computer-based design optimization technique for minimizing the structural cost of general tall buildings subject to static and dynamic serviceability design criteria. Once the wind-induced dynamic response of a tall building structure is accurately determined and the optimal serviceability design problem is explicitly formulated, a rigorously derived Optimality Criteria (OC) method is to be developed to achieve the optimal distribution of element stiffness of the structural system satisfying the wind-induced drift and acceleration design constraints. The effectiveness and practicality of the optimal design technique are illustrated by a full-scale 60-story building with complex 3D mode shapes. Both peak resultant acceleration criteria and frequency dependent modal acceleration criteria are considered and their influences on the optimization results are highlighted. Results have shown that the use of various acceleration criteria has different implications in the habitability evaluations and subsequently different optimal design solutions. The computer based optimization technique provides a powerful tool for the lateral drift and occupant comfort design of tall building structures.

Keywords: serviceability design; occupant comfort criteria; stiffness optimization; dynamic analysis; optimality criteria method.

1. Introduction

Recent trends towards developing increasingly taller and irregularly shaped buildings have led to slender complex structures that are highly sensitive and susceptible to wind-induced vibration. When today's tall buildings continue to increase in height, the occupant comfort or habitability evaluation of tall buildings becomes a more critical serviceability consideration in the structural design process. In the design of such a new generation of tall buildings, structural engineers are facing the challenge of striving for the most efficient and economical design solution while ensuring that the final design must be serviceable for its intended function and safe over its design life-time. Therefore, there is a need to develop an integrated wind-induced dynamic analysis and automated computer-based design optimization technique for minimizing the structural cost of tall buildings subject to dynamic serviceability design criteria.

* Corresponding Author, Associated Professor, E-mail: cecmchan@ust.hk

Given the design wind speed for any recurrence interval, wind-induced responses of buildings could be predicted by accurate analysis of wind loads and their effects on building structures. Contemporary tall buildings having complex geometric shapes accompanied by non-coincident centers of mass and resistance may vibrate in a lateral-torsional manner, thus making the prediction of wind-induced responses of such buildings more difficult than that of regular symmetric buildings with simple geometric shapes and uncoupled one-dimensional (1D) mode shapes (Tallin and Ellingwood 1985, Kareem 1985, Yip and Flay 1995, Chen and Kareem 2005a). For the past few decades, wind-tunnel testing has been the best practice to measure wind loads and estimate wind-induced effects on tall buildings (Cermak 2003). By means of either the high-frequency force balance (HFFB) or synchronous multi-pressure sensing system (SMPSS), aerodynamic wind loads can be estimated experimentally on a rigid scaled model of the prototype. Based on the measured aerodynamic wind load, the dynamic response of a building system can then be analyzed in the time or frequency domain. In recent years, the dynamic analysis of wind-induced lateral-torsional motion of asymmetric buildings has been studied in the frequency domain by a number of researchers (Tallin and Ellingwood 1985, Kareem 1985, Islam *et al*. 1992, Yip and Flay 1995, Huang *et al*. 2009). Chen and Kareem (2005a) presented a new systematic framework for dynamic analyses of three-dimensional (3D) coupled wind-induced responses of buildings. Using this framework, equivalent static wind loads (ESWLs) can be readily determined and the dynamic response of a building can be represented in the mean, background and resonant components.

To ensure serviceable condition for a tall building, the serviceability limit states on lateral drift and acceleration should be checked. The extreme wind loading conditions of a 50-year return period are generally used for checking the serviceability lateral drift criteria and safety requirements. It has been widely accepted that the perception of wind-induced motion is closely related to the acceleration response of buildings (Kwok *et al*. 2007). Both standard deviation acceleration and peak acceleration under extreme wind conditions of 1-year, 5-year or 10-year return period are commonly used for evaluating wind induced motions experienced in tall buildings (Burton *et al*. 2007). Frequency dependent motion perception criteria in terms of 5-year-recurrence standard deviation acceleration have been established in the International Standards Organization 6897 (ISO 1984) for low frequency motion within the range of 0.063 to 1 Hz. Peak acceleration criteria associated with the extreme wind events have also been established in a number of modern design codes to preclude discomfort of occupants due to fear for safety in extreme windstorm or typhoon events. For example, the peak acceleration criteria of 15 milli-g for residential buildings and 25 milli-g for commercial buildings under 10-year return period of wind conditions are recommended in the National Building Code of Canada (NBCC 1995), the Chinese code (JGJ 3-2002), and the Hong Kong Codes of Practice (HKCOP 2004, HKCOP 2005). The Architectural Institute of Japan Guidelines for the Evaluation of Habitability (AIJ-GEH 2004) provides frequency dependent peak acceleration criteria for evaluating wind-induced building vibration. The AIJ-GEH criteria established based on experimental motion simulator investigations specifies frequency dependent peak accelerations of one-year recurrence of wind, which is believed to be more closely related to frequently occurring occupant comfort conditions. A new ISO standard 10137 has also been published dealing with serviceability criteria for buildings subjected to vibrations. The frequency dependent peak acceleration criteria similar to AIJ-GEH (2004) have been adopted in ISO-10137.

Although it has long been realised that serviceability design in tall buildings is very important, research on developing systematic procedures for serviceability performance design has not received as much attention as those for ultimate strength design. Previous studies have indicated that wind-

induced vibrations can be reduced by changing the building shape to maintain better aerodynamic stability, by adding the building mass and damping, or by increasing the lateral stiffness of the building (Vickery *et al*. 1983, Banavalkar 1990, Griffis 1993). In practice, the building shape is, however often dictated by architectural aesthetics; it is hardly justifiable to increase the mass of the building and it has not been common to design damping into a building. A rational approach for offering a permanent solution to suppressing wind-induced motions is to provide the stiffest possible structural system to the building.

The search for the optimal structural design for a tall building to meet various static and dynamic serviceability criteria is generally a rather difficult and laborious task. The current design practice through trial and error relies heavily on the structural engineer's experience and intuition, thus resulting in final design that may be feasible but not necessarily optimal. Numerical structural optimization has long been recognized as a powerful approach to automatically seek the most cost efficient design while satisfying all specified design performance criteria. Recently, an effective design optimization approach has been developed for stiffness design optimization of tall buildings with uncoupled mode shapes (Chan and Chui 2006, Chan *et al*. 2007). Chan and Chui (2006) presented an occupant comfort serviceability design optimization technique for uncoupled symmetric tall steel buildings subject to the ISO-6897's standard deviation acceleration criteria. Chan *et al*. (2007) developed an integrated optimal design framework that couples together an aerodynamic wind load updating process and a drift design optimization algorithm for symmetric tall building structures. Although these studies represent recent advances in the use of structural optimization techniques for serviceability designs of tall buildings, it is necessary to extend the applications of the optimal stiffness design technique to general asymmetric tall buildings subject to multiple wind induced drift and acceleration constraints.

In this paper, an automated stiffness optimization technique for the serviceability design of tall general buildings is presented. The lateral static drift and dynamic peak and standard deviation acceleration responses of an asymmetric tall building are analyzed under various levels of return period of wind loading. The optimal stiffness design problem of the building subject to drift and both peak and standard deviation acceleration constraints is explicitly formulated in terms of element sizing design variables. A rigorously derived Optimality Criteria method, which has been shown to be particularly suitable for large element sizing optimization problems, is employed to solve the optimal stiffness design problem. Finally, a full-scale 60-story asymmetric building with 3D coupled mode shapes is used to demonstrate the applicability and effectiveness of the automated stiffness design optimization technique.

2. Response analysis of wind-induced motion

Since wind excitation is generally regarded as a stationary and ergodic random process, it is more convenient to conduct wind-induced response analysis in the frequency domain. Using the HFFB or SMPSS technique, aerodynamic wind loads on a building can be measured in a boundary-layer wind tunnel, after which the dynamic response of the building can be calculated for any combination of the building's mass, stiffness and damping ratio. Based on random vibration theory, the power spectral density (PSD) matrix of the displacement response vector can be calculated in the frequency domain as

$$[S_s(f)] = \mathbf{\Phi H}(f)\mathbf{\Phi}^T[S_{F_{sl}}(f)]\mathbf{\Phi H}^*(f)\mathbf{\Phi}^T, \ (s, l = x, y, \theta) \tag{1}$$

where $\mathbf{\Phi}$ = the mode shape matrix for n modes of the building; $S_{F_{sl}}$ = the input aerodynamic wind load spectra which can be derived from the measured wind tunnel time history loading data; $\mathbf{H}(f) = diag\left[\frac{1}{m_j(2\pi f_j)^2}H_j(f)\right]$ = the matrix of the system frequency response functions; and $\mathbf{H}^*$ = the complex conjugate of $\mathbf{H}$. The diagonal elements of the matrix $\mathbf{H}$ are known as the modal frequency response function (or referred as the mechanical admittance function), which can be expressed as a non-dimensional complex function as

$$H_j(f) = \frac{1}{1-(f/f_j)^2 + 2i\xi_j f/f_j}, \ j = 1, 2, \ldots, n \tag{2}$$

in which f_j = the j-th modal frequency; ξ_j = the j-th modal damping ratio. Using the, so called, full spectral approach given in Eq. (1), the PSD function of the physical displacements considering all auto and cross modal correlations can be accurately determined.

Given the s component of n number of 3D mode shapes of the building system at elevation z, i.e., $\{\phi_s(z)\}^T = \{\phi_{1s}(z), \phi_{2s}(z), \ldots, \phi_{ns}(z)\}$, the mean square value of the s-th component displacement response of the building system at elevation z can be given as

$$\sigma_s^2 = \sum_{j=1}^{n}\phi_{js}^2(z)\sigma_{q_{jj}}^2 + \sum_{j=1}^{n}\sum_{\substack{k=1\\ j\neq k}}^{n}\phi_{js}(z)\phi_{ks}(z)r_{jk}\sigma_{q_{jj}}\sigma_{q_{kk}}, \quad (s = x, y, \theta) \tag{3}$$

where $\sigma_{q_{jj}}^2$ represents the variance or mean square value of the j-th modal displacement response; and r_{jk} denoting the intermodal correlation coefficient can be defined as

$$r_{jk} = \frac{C_{q_{jk}}}{\sigma_{q_{jj}}\sigma_{q_{kk}}} = \frac{Re\left[\int_0^\infty H_j(f)S_{Q_{jk}}(f)H_k^*(f)df\right]}{\sqrt{\int_0^\infty H_j^2(f)S_{Q_{jj}}(f)df}\sqrt{\int_0^\infty H_k^2(f)S_{Q_{kk}}(f)df}} \tag{4}$$

where $C_{q_{jk}}$ = the covariance between the j-th and k-th modal displacement responses; $S_{Q_{jj}}$ = the power spectral density of the j-th modal force $Q_j(t)$; $S_{Q_{jk}}$ = the cross power spectral density (XPSD) between $Q_j(t)$ and $Q_k(t)$. The proper evaluation of the intermodal correlation coefficient r_{jk} can be referred to the recent work of Chen and Kareem (2005b) and Huang *et al*. (2009).

Similarly, the s-th component acceleration response can also be written by combining the modal acceleration response as

$$\sigma_{\ddot{s}}^2 = \sum_{j=1}^{n}\phi_{js}^2(z)\sigma_{\ddot{q}_{jj}}^2 + \sum_{j=1}^{n}\sum_{\substack{k=1\\ j\neq k}}^{n}\phi_{js}(z)\phi_{ks}(z)r_{jk}\sigma_{\ddot{q}_{jj}}\sigma_{\ddot{q}_{kk}}, \quad (s = x, y, \theta) \tag{5}$$

where $\sigma_{\ddot{q}_{jj}}^2$ representing the variance or mean square value of the j-th modal acceleration response

can be given as

$$\sigma^2_{\ddot{q}_{jj}} = \frac{\int_0^\infty (2\pi f)^4 |H_j(f)|^2 S_{Q_{jj}}(f) df}{m_j^2 (2\pi f_j)^4} \tag{6}$$

where m_j = the j-th modal mass. Assuming that the generalized wind force spectra as white noise, the modal acceleration response could be approximated from Eq. (6) as (Tallin and Ellingwood 1985)

$$\sigma^2_{\ddot{q}_{jj}} \approx \frac{\pi f_j}{4\xi_j m_j^2} S_{Q_{jj}}(f_j) \tag{7}$$

Once the covariance matrix for the acceleration response at the reference center has been determined, the total resultant acceleration incorporating both swaying and torsional effects experienced at a distance from the reference center of the top floor can then be estimated. For instance, the total translational component acceleration at the most distant corner (R_x, R_y) from the reference center of a building can be given as

$$a_{cx}(t) = \ddot{x}(t) - R_y \ddot{\theta}(t), \quad a_{cy}(t) = \ddot{y}(t) + R_x \ddot{\theta}(t) \tag{8}$$

where $\ddot{x}, \ddot{y}$ = the two perpendicular translational acceleration components and $\ddot{\theta}$ = the torsional acceleration component at the reference center of the building. It should be noted that Eq. (8) has been expressed in the time domain with simultaneous components of translation and torsion. With the assumption of a rigid diaphragm for each floor of the building, the most critical peak resultant acceleration can be evaluated at the most distant corner from the center of twist or the center of the rigid diaphragm at the top floor.

The resultant root-mean-square (RMS) response acceleration, σ_a, at the corner point can be calculated as follows

$$\sigma_a = \sqrt{\sigma^2_{\ddot{x}} + \sigma^2_{\ddot{y}} + (R_x^2 + R_y^2)\sigma^2_{\ddot{\theta}} - 2R_y \sigma^2_{\ddot{x}\ddot{\theta}} + 2R_x \sigma^2_{\ddot{y}\ddot{\theta}}} \tag{9}$$

where $\sigma^2_{\ddot{x}}, \sigma^2_{\ddot{y}}$ = the variance of the two translational acceleration components and $\sigma^2_{\ddot{\theta}}$ = the torsional acceleration component, all of which can be calculated using Eq. (5); $\sigma^2_{\ddot{x}\ddot{\theta}}$ =covariance of $\ddot{x}$ and $\ddot{\theta}$; and $\sigma^2_{\ddot{y}\ddot{\theta}}$, = covariance of $\ddot{y}$ and $\ddot{\theta}$.

When the correlations between any two component motions in the x, y and θ directions are small, the covariance terms $R_y \sigma^2_{\ddot{x}\ddot{\theta}}$ and $R_x \sigma^2_{\ddot{y}\ddot{\theta}}$ are small as compared with the other three variance terms such that the RMS resultant acceleration may be simplified to the following form as

$$\sigma_a \approx \sqrt{\sigma^2_{\ddot{x}} + \sigma^2_{\ddot{y}} + (R_x^2 + R_y^2)\sigma^2_{\ddot{\theta}}} \tag{10}$$

The maximum peak acceleration response $a\tau$ over a given time duration τ, is an important measure for assessing occupant comfort serviceability. The expected value of the largest peak response at the top corner of the building, can be expressed by

$$\sigma_\tau \approx g_f \sqrt{\sigma^2_{\ddot{x}} + \sigma^2_{\ddot{y}} + (R_x^2 + R_y^2)\sigma^2_{\ddot{\theta}}} \tag{11}$$

where g_f = the peak factor. For a Gaussian process, the peak factor g can be given as follows

(Davenport 1964)

$$g_f = \sqrt{2\ln v\tau} + 0.5772/\sqrt{2\ln v\tau} \tag{12}$$

where v denoting the mean zero-crossing rate of the acceleration process can be approximated as the modal frequency of a building, and τ representing the observation time duration for assessing acceleration response may be normally taken as 600 s.

The use of Eq. (11) may generally overestimate the peak resultant acceleration, since Eq. (11) involves an underlying assumption of the coincident occurrence of the maximum translational acceleration components. In the pursuit of a better estimate, the partial dependence among the directional maximum component accelerations should be considered. Based on experimental data derived from wind tunnel tests and full-scale measurements taken at the Boundary Layer Wind Tunnel Laboratory, Isyumov (1982, 1992) developed an empirical relationship between the maxima of two independent component responses or commonly referred to as the joint action factor φ. In general the joint action factor has a value ranging between 0.7 and 1, depending on the ratio of the smaller component to the larger component response. A larger value of the ratio of two component responses implies a smaller value of the joint action factor, or vice versa. A more realistic resultant peak acceleration of a tall building can be computed by multiplying together the overestimated value given by Eq. (11) and the joint action factor as

$$\hat{a}_c \approx \varphi g_f \sqrt{\sigma_{\ddot{x}}^2 + \sigma_{\ddot{y}}^2 + (R_x^2 + R_y^2)\sigma_{\ddot{\theta}}^2} \tag{13}$$

For a building with weakly coupled inter-component acceleration responses, one of the two translational acceleration components may dominate the building motion at the corner such that the joint action factor becomes close to 1 (Isyumov *et al*. 1992).

Substituting Eq. (5) into Eq. (13) and rearranging terms, the peak resultant acceleration can be written as

$$\hat{a} = \varphi g_f \sqrt{\sum_{j=1}^{n} \sum_{s=x,y,\theta} \tilde{\phi}_{js}^2 \sigma_{\ddot{q}_{jj}}^2 + \sum_{j=1}^{n} \sum_{\substack{k=1 \\ j \neq k}}^{n} \sum_{s=x,y,\theta} \tilde{\phi}_{js}\tilde{\phi}_{ks} r_{jk} \sigma_{\ddot{q}_{jj}} \sigma_{\ddot{q}_{kk}}} \tag{14}$$

in which the transformed swaying mode shapes at the most distant corner of the top floor of the building are given as

$$\tilde{\phi}_{jx} = \phi_{js}(H);\ \tilde{\phi}_{jy} = \phi_{jy}(H);\ \tilde{\phi}_{j\theta} = \sqrt{R_x^2 + R_y^2} \times \phi_{j\theta}(H) \tag{15}$$

where H = the height of the building and (R_x,R_y) = the planar position of the most distant corner at the top floor of the building.

Eq. (14) gives a good approximation of peak resultant acceleration response, particularly for a tall building with weakly inter-component coupling effects. However, it is worth noting that there are some inherent shortcomings in Eq. (14). The peak factor in Eq. (14) is calculated with the mean crossing rate simply approximated by the first modal frequency of a building. A more realistic peak factor is needed mode by mode for the resultant acceleration, which is related to multiple modes rather than only the first mode. Using the modal frequency f_j to approximate the mean zero-crossing rate in Eq. (12), the modal peak factor g_{f_j} can then be calculated by Eq. (12) for each vibration

mode of a tall building. With the aid of g_{f_j}, Eq. (14) can then be improved by considering actual peak factors in different modes as

$$\hat{a}= \varphi \sqrt{\sum_{j=1}^{n} \sum_{s=x,y,\theta} g_{f_j}^2 \phi_{js}^2 \sigma_{q_{jj}}^2 + \sum_{j=1}^{n} \sum_{k=1}^{n} \sum_{\substack{s=x,y,\theta \\ j \neq k}} g_{f_j} g_{f_k} \tilde{\phi}_{js} \tilde{\phi}_{ks} r_{jk} \sigma_{\ddot{q}_{jj}} \sigma_{\ddot{q}_{kk}}} \tag{16}$$

3. Occupant comfort criteria

Much research effort has been devoted to investigate human perception and tolerance thresholds of wind-induced building motion since 1970s (Hansen *et al*. 1973, Irwin 1978, Lee 1983, Isyumov *et al*. 1988, Goto *et al*. 1990, Melbourne and Palmer 1992, Isyumov and Kilpatrick 1996). Although some recommendations on acceleration limitations have been given in a number of current design codes, there is still no internationally well accepted standard for limiting wind-induced motion in buildings. The research on perception evaluation of wind-induced vibration in buildings is still an active research topic in wind engineering (Tamura *et al*. 2006, Burton *et al*. 2006, 2007, Kwok *et al*. 2007, 2009).

There has long been debate about whether human response to wind-induced motion is dependent on the frequency of motion. Chang (1967, 1973) was one of the first to suggest frequency independent occupant comfort criteria based on observations on actual buildings. The first codified recommendations suggesting frequency independent peak acceleration criteria were given in the National Building Code of Canada 1977. Based on the review of a large amount of work (Chen and Robertson 1973, Hansen *et al*. 1973) regarding many aspects of human response to vibration, field measurements and interviews of occupants, Irwin (1978) showed frequency dependence of uniaxial sinusoidal motion and recommended frequency dependent acceleration criteria for evaluating low-frequency motion within the range of 0.063 Hz to 1.0 Hz, which later led to the development of the ISO-6897 guidelines (ISO 1984). The ISO-6897's motion perception threshold expressed in terms of standard deviation acceleration for a 10-minute duration in 5-year-recurrence wind is given as a function of frequency as

$$\sigma_{\ddot{q}_{jj}}^{U} = \exp(-3.65 - 0.41 \ln f_j) \tag{17}$$

where $\sigma_{\ddot{q}_{jj}}^{U}$ denotes the threshold of standard deviation modal acceleration.

In current design practice, it appears that standard deviation acceleration and peak acceleration are two important measures for assessing human perception of building motion. Since the human perception may be more dominated by the overall averaged effect for long duration events of a stationary vibration, using the standard deviation acceleration may be a reasonable choice to check the occupant comfort performance of buildings under more frequently occurring wind events (Boggs 1995, Burton *et al*. 2007). But for short duration infrequently occurring extreme wind events, such as thunderstorms and typhoons, averaging the acceleration over the worst 10-minutes of the non-stationary motion of buildings may be statistically meaningless, and may also underestimate the effects of the largest individual peaks, whereby occupants are likely in alarm with fear for safety (Burton *et al*. 2007). It seems that the two kinds of acceleration response (peak acceleration and standard deviation acceleration) may characterize different motion effects on human response. In

practice, the choice of a particular acceleration criterion for a building may depend on not only the type of dominating wind events in a geographical location, but also whether it is the perception threshold or actual discomfort which is being evaluated.

Although recent studies have indicated that the evaluation of occupant comfort in buildings should include frequency dependency of motion (Burton *et al*. 2006, 2007), the incorporation of the frequency dependent modal acceleration criteria into the serviceability design of tall buildings involving complex modes of vibration is problematic. For asymmetric tall buildings with complex 3D mode shapes, the acceleration response should constitute the combination of all significant modal acceleration responses as shown in Eq. (5). While it may be more accurate to include all contributory modes of vibration in the prediction of wind-induced acceleration response of the building, it is not clear, however, whether the acceleration response should be checked against the modal acceleration criteria based on the first mode or a combination of all contributory modes. Furthermore, it is questionable whether the total motion resulting from all contributory modes of vibration may be fully sensed by general occupants. As opposed to the frequency dependent modal acceleration criteria, the frequency independent peak acceleration criteria provide a convenient alternative for checking the acceptability of wind-induced motion in complex tall buildings. Once the resultant acceleration response taking full account of combined swaying and torsional effects at the critical location of a building is determined, its value can then be conveniently checked against a fixed acceleration threshold.

Upon the establishment of wind-induced drift and acceleration criteria, the optimal serviceability design problem can then be mathematically formulated in terms of design variables. In assessing the serviceability performance of modern complex tall buildings, it is necessary to develop a general design optimization framework, which encompasses various kinds of static and dynamic design performance constraints. Various occupant comfort design criteria ranging from modal acceleration criteria corresponding to more frequently occurring wind conditions and peak resultant acceleration criteria associated with less frequently occurring extreme wind events should be included in the design optimization framework as different design requirements under various serviceability performance levels.

4. Wind-induced serviceability design optimization

Consider a general tall building having $i_s = 1,2, \ldots, N_s$ steel frame elements, $i_c = 1,2, \ldots, N_c$ concrete frame elements and $i_w = 1,2, \ldots, N_w$ concrete shear wall elements. The design problem of minimizing the material cost of a tall building structure subject to a set of serviceability design constraints including the static drift and the peak resultant acceleration, standard deviation modal acceleration as well as peak modal acceleration design criteria can be posed as

Minimize

$$W(A_{i_s}, B_{i_c}, D_{i_c}, t_{i_w}) = \sum_{i_s=1}^{N_s} w_{i_s} A_{i_s} + \sum_{i_c=1}^{N_c} w_{i_c} B_{i_c} D_{i_c} + \sum_{i_w=1}^{N_w} w_{i_w} t_{i_w} \tag{18}$$

Subject to

$$d_l \le d_l^U \qquad (l=1,2,\ldots,N_l) \tag{19}$$

$$\hat{a}_l \le a_l^U \qquad (l=1,2,\ldots,N_l) \tag{20}$$

$$\sigma_{\ddot{q}_{jj}} \le \sigma_{\ddot{q}_{jj}}^U \qquad (j=1,2,\ldots,n) \tag{21}$$

$$g_{f_j}\sigma_{\ddot{q}_{jj}} \le a_{\ddot{q}_{jj}}^U \qquad (j=1,2,\ldots,n) \tag{22}$$

$$A_{i_s}^L \le A_{i_s} \le A_{i_s}^U \qquad (i_s=1,2,\ldots,N_s) \tag{23}$$

$$B_{i_c}^L \le B_{i_c} \le B_{i_c}^U \qquad (i_c=1,2,\ldots,N_c) \tag{24}$$

$$D_{i_c}^L \le D_{i_c} \le D_{i_c}^U \qquad (i_c=1,2,\ldots,N_c) \tag{25}$$

$$t_{i_w}^L \le t_{i_w} \le t_{i_w}^U \qquad (i_w=1,2,\ldots,N_w) \tag{26}$$

Eq. (18) defines the objective function of the minimum material cost, in which $w_{i_s}, w_{i_c}, w_{i_w}$ = the respective unit cost of the steel sections, concrete sections and shear walls; A_{i_s} = cross section area of steel section i_s; B_{i_c}, D_{i_c} = width and depth of rectangular concrete section i_c; and t_{i_w} = thickness of concrete wall section i_w. Eq. (19) represents the lateral displacement or interstory drift constraints under equivalent static 50-year return period wind loading for $l = 1, 2, \ldots, N_l$ incident wind directions and d_l^U = the allowable displacement or interstory drift ratio limit. In general, the allowable wind-induced drift ratio for tall buildings appears to be within the range of 1/750 to 1/250, with 1/400 being typical. Eq. (20) represents the set of peak resultant acceleration constraints under a typical 10-year return period wind for $l = 1, 2, \ldots, N_l$ incident wind directions, where $\hat{a}_l$ = peak resultant acceleration; and $\hat{a}_l^U$ = the corresponding l-th predefined acceleration limiting value. Eq. (21) gives the dynamic serviceability constraints in terms of the standard deviation modal acceleration according to the ISO-6897 criteria for a 10-minute duration in 5-year return period wind. Eq. (22) represents the peak modal acceleration constraints based on the AIJ-GEH criteria for a 10-minute duration in 1-year period return wind, where g_{f_j} denoting a modal peak factor can be obtained from Eq. (12). Eq. (23) to Eq. (26) define the element sizing bounds in which superscript L denotes lower size bound and superscript U denotes upper size bound of member i.

In the acceleration constraints from Eq. (20) to Eq. (22), the acceleration response with a given recurrence interval can be evaluated based on individual directions. Actually, the N-year-recurrence acceleration is defined on a certain probability of exceedence regardless of wind directions, and should be calculated by integrating all directional probability of occurrence. Since the directionality information of design wind speed is generally not available, the N-year-recurrence acceleration responses are respectively evaluated for each direction with a uniform non-directional N-year-recurrence design wind speed in this paper.

Eqs. (21) and (22) provide a simplified way to evaluate the frequency-dependent acceleration criteria in terms of modal values. It is worth noting that the mode-by-mode checking of ISO and AIJ-GEH criteria may not be reasonable when the building under consideration has closely spaced modal frequencies. In such a case, the RMS combined resultant acceleration rather than the modal value should be used to check against the frequency-dependent occupant comfort criteria. Similar to the peak resultant acceleration constraints, the RMS combined acceleration constraints can also be formulated into the proposed stiffness design optimization technique. However, due to paper length limitation, the formal treatment of the RMS resultant acceleration constraint has not been given in this paper.

For practical design purpose, the dynamic wind forces can be treated as equivalent static loads. Based on wind-induced response analysis presented earlier, the equivalent static wind loads can be

obtained and expressed in terms of the alongwind, crosswind and torsional directional loads. Each directional loading consists of the mean, the background and the resonant components. A comprehensive framework for determining the ESWLs on tall buildings can be referred to the recent literature (e.g., Chen and Kareem 2005a, Chan *et al*. 2007). A major difference between optimizing for static loads and equivalent static wind loads is the fact that ESWLs are indeed dependent upon the natural frequency of the building. Since the natural frequency of a building is a function of its structural stiffness and mass, making a change in the element sizes of the building may also lead to a change in the value of the ESWLs. In order to make an accurate prediction of the wind-induced drift response under the actions of ESWLs at the time of the structural design phase, it is necessary that the ESWLs be instantaneously updated whenever there exists a significant change in the structural properties of the building (Chan *et al*. 2009).

4.1 Explicit formulation of drift and acceleration constraints

To facilitate a numerical solution of the design optimization problem, it is necessary that the implicit drift and acceleration constraints through Eq. (19) to Eq. (22) be formulated explicitly in terms of design variables. Using the principle of virtual work, the elastic drift response of a building under the actions of ESWLs can be explicitly expressed as (Chan 2001)

$$d_l(A_{i_s}, B_{i_c}, D_{i_c}, t_{i_w}) = \sum_{i_s=1}^{N_s}\left(\frac{e_{i_s j}}{A_{i_s}} + e'_{i_s j}\right) + \sum_{i_c=1}^{N_c}\left(\frac{e_{0i_c j}}{B_{i_c} D_{i_c}} + \frac{e_{1i_c j}}{B_{i_c} D_{i_c}^3} + \frac{e_{2i_c j}}{B_{i_c}^3 D_{i_c}}\right) + \sum_{i_w=1}^{N_w}\left(\frac{e_{0i_w j}}{t_{i_w}} + \frac{e_{1i_w j}}{t_{i_w}^3}\right) \le d_j^U \quad (l = 1, \ldots, N_l) \tag{27}$$

where $e_{i_s j}$ and $e'_{i_s j}$ are the virtual strain energy coefficient and its correction factor of steel members respectively; $e_{0i_c j}$, $e_{1i_c j}$ and $e_{2i_c j}$ are the virtual strain energy coefficients of concrete frame members; and $e_{0i_w j}$, $e_{1i_w j}$ are the virtual strain energy coefficients of concrete wall members. Once the finite element analysis is carried out for a given structural design under the ESWLs and virtual loading conditions, the internal element forces and moments are obtained and the element's virtual strain energy coefficients can then be readily calculated.

With the aid of piece-wise regression analysis, the PSD function of modal wind forces for a typical tall building can be inversely related to the modal frequency of the building and is expressed as an algebraic function of the frequency within the typical range of frequency for dynamic serviceability check as follows (Chan and Chiu 2006)

$$S_{Q_{jj}}(f_j) = \beta_j f_j^{-\alpha_j} \tag{28}$$

where α_j and β_j are regression constants and normally $\alpha_j > 1$ and $\beta_j > 0$. Substituting Eq. (28) into Eq. (7) gives

$$\sigma_{\ddot{q}_{jj}}^2 \approx \frac{\pi}{4\xi_j m_j^2}\beta_j f_j^{-(\alpha_j - 1)} \tag{29}$$

For wind sensitive tall buildings where the value of the exponent α_j is normally larger than 1, the modal acceleration response can be reduced according to Eq. (29) by increasing the modal frequency or the modal stiffness if the modal mass is assumed to be constant. Since the self weight of the lateral load resisting system contribute only a small part of the entire building mass, which includes mostly the dead loads of floor slabs, structural and non-structural components, as well as the occupancy live loads, the building stiffness is usually more affected by resizing the lateral load resisting elements with insignificant changes in the total building mass. Therefore, the assumption of constant building mass can be reasonably adopted in this design optimization technique for convenience.

It is worth noting that some special tall buildings with well organized aerodynamic shapes may result in a flat modal force spectrum with $\alpha_j \approx 1$ over an extended range of frequencies. In such special cases, the dynamic responses become insensitive to any change in the modal frequency of such buildings and some other measures, such as adding mechanical dampers, may become necessary to mitigate wind-induced vibration. In practice, a flat nondimensional spectrum is only found within a limited frequency range near the vortex shedding peak. Then the stiffness optimization technique can still be effectively used to reduce acceleration.

Substituting Eq. (29) into Eq. (16), the peak resultant acceleration can be explicitly expressed in terms of n modal frequencies as

$$\hat{a} \approx \varphi \frac{\sqrt{\pi}}{2} \left[\sum_{j=1}^{n} \sum_{s=x,y,\theta} g_{f_j} \tilde{\phi}_{js}^2 \frac{\beta_j f_j^{-(\alpha_j-1)}}{\xi_j m_j^2} + \sum_{j=1}^{n} \sum_{k=1}^{n} \sum_{\substack{s=x,y,\theta \\ j \neq k}} g_{f_j} g_{f_k} \tilde{\phi}_{js} \tilde{\phi}_{ks} \frac{r_{jk}}{m_j m_k} \sqrt{\frac{\beta_j \beta_k f_j^{-(\alpha_j-1)} f_k^{-(\alpha_k-1)}}{\xi_j \xi_k}} \right]^{1/2} \tag{30}$$

Using the Rayleigh Quotient method, the modal frequency f_j or natural period T_j of a building system can be related to the total internal strain energy U_j of the structural system due to the j-th modal inertia force applied statically to the system as follows (Huang and Chan 2007)

$$U_j = c_j / f_j^2 = c_j T_j^2 \tag{31}$$

where c_j denotes a proportionality constant relating the j-th modal internal strain energy U_j to the square of the corresponding modal frequency f_j or the square of the modal period T_j of the system. Substituting Eq. (31) into Eq. (30), the peak resultant acceleration constraints given in Eq. (20) can be expressed as a function of the total internal strain energy of the system U_j as follows

$$\hat{a}_l = \varphi \frac{\sqrt{\pi}}{2} \left[\sum_{j=1}^{n} \sum_{s=x,y,\theta} g_{f_j} \tilde{\phi}_{js}^2 A_j (U_j)^{\frac{\alpha_j-1}{2}} + \sum_{j=1}^{n} \sum_{k=1}^{n} \sum_{s=x,y,\theta} g_{f_j} g_{f_k} \tilde{\phi}_{js} \tilde{\phi}_{ks} B_{jk} (U_j)^{\frac{\alpha_k-1}{4}} (U_k)^{\frac{\alpha_k-1}{4}} \right]^{1/2} \leq a_l^U \tag{32}$$
$$j \neq k$$

where the constants A_j and B_{jk} can be given as

$$A_j = \frac{\beta_j}{\xi_j m_j^2} \left(\frac{1}{c_j} \right)^{\frac{\alpha_j-1}{2}}; \quad B_{jk} = \frac{r_{jk}}{m_j m_k} \sqrt{\frac{\beta_j \beta_k}{\xi_j \xi_k}} \left(\frac{1}{c_j} \right)^{\frac{\alpha_j-1}{4}} \left(\frac{1}{c_k} \right)^{\frac{\alpha_k-1}{4}} \tag{33}$$

Similarly, both the standard deviation modal acceleration and peak modal acceleration values given in the occupant comfort design constraints of Eqs. (21) and (22) can also be expressed in terms of the modal internal strain energy of the system U_j as follows

$$\sigma_{\ddot{q}_{jj}} \approx \left[\frac{\pi}{4\xi_j m_j^2}\beta_j\left(\frac{c_j}{U_j}\right)^{-\frac{\alpha_j-1}{2}}\right]^{1/2} = \frac{\sqrt{\pi}}{2}\left[A_j(U_j)^{\frac{\alpha_j-1}{2}}\right]^{1/2} \tag{34}$$

$$g_{f_j}\sigma_{\ddot{q}_{jj}} \approx \left[\sqrt{\ln\tau^2\left(\frac{c_j}{U_j}\right)} + 0.5772/\sqrt{\ln\tau^2\left(\frac{c_j}{U_j}\right)}\right]\frac{\sqrt{\pi}}{2}\left[A_j(U_j)^{\frac{\alpha_j-1}{2}}\right]^{1/2} \tag{35}$$

The frequency dependent standard deviation modal acceleration thresholds involved in Eq. (21) can be related to the modal internal strain energy as

$$\sigma^U_{\ddot{q}_{jj}} = \exp(-3.65 - 0.41\ln f_j) = \exp\left[-3.65 - 0.205\ln\left(\frac{c_j}{U_j}\right)\right] \tag{36}$$

The AIJ-GEH's peak modal acceleration threshold corresponding to the 90% perception probability for office buildings involved in Eq. (22) can be approximated by the following expression (Kwok *et al*. 2007) as

$$a^U_{\ddot{q}_{jj}} = 3.5*0.72*\exp(-3.65 - 0.41\ln f_j) = 3.5*0.72*\exp\left[-3.65 - 0.205\ln\left(\frac{c_j}{U_j}\right)\right] \tag{37}$$

where the value of 3.5 is a typical value of the peak factor; 0.72 is a multiplication factor as recommended by ISO-6897 (1984), which converts the limiting acceleration from a recurrence interval of five years to one year. It should be noted that the AIJ-GEH frequency dependent peak acceleration criterion in Eq. (37) is similar to the comfort criteria for office buildings in ISO-10137 (2007).

For a tall building of mixed steel and concrete construction, the total internal strain energy U_j of the building structure can be obtained by first analyzing statically the structure under the application of modal inertia loads and then summing up the internal work done of each member as

$$\begin{aligned} U_j(A_{i_s}, B_{i_c}, D_{i_c}, t_{i_w}) = & \sum_{i_s=1}^{N_s}\left(\frac{e_{i_s j}}{A_{i_s}} + e'_{i_s j}\right) + \sum_{i_c=1}^{N_c}\left(\frac{e_{0i_c j}}{B_{i_c}D_{i_c}} + \frac{e_{1i_c j}}{B_{i_c}D^3_{i_c}} + \frac{e_{2i_c j}}{B^3_{i_c}D_{i_c}}\right) \\ & + \sum_{i_w=1}^{N_w}\left(\frac{e_{0i_w j}}{t_{i_w}} + \frac{e_{1i_w j}}{t^3_{i_w}}\right) \qquad (l = 1, 2\ldots n) \end{aligned} \tag{38}$$

where $e_{i_s j}, e'_{i_s j}$ = the internal strain energy coefficients and its correction factor of steel member i_s; $e_{0i_c j}, e_{1i_c j}, e_{2i_c j}$ = the internal strain energy coefficients of concrete member i_c; and $e_{0i_w j}, e_{1i_w j}$ the internal strain energy coefficients of concrete wall section i_w. Note that the total strain energy expression (Eq. (41)) relating to the modal frequency of the building system looks very similar to

the virtual strain energy expression (Eq. (28)) relating to the static wind drift response of the system. The only difference is that the strain energy expression given in Eq. (41) is derived from the static analysis of the structure under the application of the modal inertia forces, whereas the energy expression Eq. (27) is derived from the static analysis of the structure due to the application of the actual ESWLs and virtual load cases.

4.2 Optimality criteria method

Upon establishing the explicit formulation of the drift and various kinds of acceleration design constraints, the next task is to apply a suitable numerical technique for solving the optimal serviceability design problem. A rigorously derived Optimality Criteria (OC) method, which has been shown to be computationally efficient for large-scale structures is herein employed (Chan 2001, Chan 2004). In this OC approach, a set of optimality criteria for the optimal design is first derived and a recursive algorithm is then applied to indirectly solve for the optimal solution by satisfying the derived optimality criteria.

For simplification of discussion, the optimal serviceability design problem (i.e., Eq. (18) to Eq. (26)) can be written into a generic form in terms of i= *1,2, ..., N_i* generalized member design variable X_i representing all element sizing design variables (i.e., A_{i_s}, B_{i_c}, D_{i_c} and t_{i_w}) as

Minimize
$$W(X_i) = \sum_{i=1}^{N_i} w_i X_i \tag{39}$$

subject to
$$G_j(X_i) \le 0 \qquad (j = 1, 2\ldots, N_j) \tag{40}$$

$$X_i^L \le X_i \le X_i^U \qquad (i = 1, 2\ldots, N_i) \tag{41}$$

where $G_j(X_i) \le 0$ represents the set of drift and acceleration design constraints which have been explicitly expressed in term of design variables X_i. To seek for numerical solution using the OC method, the constrained optimal design problem (i.e., Eq. (39) to Ep. (41)) must be transformed into an unconstrained Lagrangian function which involves both the objective function and the set of design constraints G_j associated with corresponding Lagrangian multipliers λ_j. By differentiating the Lagragian function with respect to each sizing design variable and setting the derivatives to zero, the necessary stationary optimality conditions can be obtained and then utilized in the following recursive relation to resize the active sizing variables (Chan 2001).

$$X_i^{v+1} = X_i^v \cdot \left\{ 1 - \frac{1}{\eta}\left(\sum_{j=1}^{N_j} \lambda_j \frac{\partial G_j / \partial X_i}{\partial W / \partial X_i} + 1 \right) \right\}_v \qquad (i = 1, 2, \ldots, N_i) \tag{42}$$

where λ_j denotes the associated Lagrangian multiplier for the j-th design constraint, v represents the current iteration number; and η is a relaxation parameter. During the resizing iteration for X_i, any member reaching its size bounds is deemed as an inactive member, and its size is set at its corresponding size limit. The two partial derivatives with respect to design variables involved in Eq. (42) could be readily obtained, since the objective function W and the drift and acceleration constraints

$G_j(X_i)$ have been explicitly expressed in terms of the design variables.

Before Eq. (42) can be applied to resize X_i, the Lagrangian multipliers λ_j must first be determined. Considering the sensitivity of the k-th constraint with respect to changes in the design variables, one can derive a set of N_j simultaneous linear equations to solve for the N_j unknown λ_j (Chan 2001)

$$\sum_{j=1}^{N_j} \lambda_j^v \left(\sum_{i=1}^{N_i} \frac{X_i \dfrac{\partial G_k}{\partial X_i} \dfrac{\partial G_j}{\partial X_i}}{\dfrac{\partial W}{\partial X_i}} \right) = -\sum_{i=1}^{N_i} \left(X_i \frac{\partial G_k}{\partial X_i} \right)_v + \eta(G_k^v) \qquad (k = 1, 2, \ldots, N_j) \tag{43}$$

Having the current design variables X_i^v, the corresponding λ_i^v values are readily determined by solving Eq. (43). Having the current values of λ_i^v, the new set of design variables X_i^{v+1} can, in turn, be obtained from Eq. (42). Therefore, the recursive application of the simultaneous equations of Eq. (43) to find the λ_j^v and the resizing formula of Eq. (42) to find the new solution of design variables constitutes the OC algorithm. By successively applying the OC algorithm until convergence occurs, the optimal design solution is then found.

4.3 Procedure of serviceability design optimization

The proposed wind-induced serviceability design optimization procedure can be outlined step by step as follows:

1. Given the geometric shape of a building, determine the aerodynamic wind load spectra and modal force spectra by wind tunnel tests and perform regression analysis on the spectral data to define the spectral curves as an algebraic function of frequency.
2. Develop the finite element model for the building and carry out an eigenvalue analysis to obtain the modal frequencies and mode shapes of the building.
3. Based on the current set of dynamic properties (i.e., natural frequencies and mode shapes) of the building, calculate the dynamic drift and acceleration responses of the building; determine the equivalent static wind loads on the building.
4. Establish the explicit expression of the drift and acceleration constraints, and explicitly formulate the dynamic serviceability design optimization problem.
5. Set up the unconstrained Lagrangian function which involves both the objective function and the set of explicit drift and acceleration constraints associated with the corresponding Lagrangian multipliers, and derive the set of optimality criteria from the stationary conditions of the Lagrangian function.
6. For the current set of element sizing design variable X_i, solve the system of simultaneous linear equations Eq. (43) for the set of Lagrange multiplier λ_j.
7. For the current value of λ_j^v, find the new set of design variables X_i^{v+1} from Eq. (42).
8. Repeat steps 6 and 7 and check the convergence of the recursive process: if all $X_i^{v+1} = X_i^v$ and $\lambda_j^{v+1} = \lambda_j^v$, then proceed to step 9.
9. Check the convergence of the design objective function: if the cost of the structure for three consecutive reanalysis-and-redesign cycles is within certain prescribed convergence criteria, for example within 0.1% difference in the structural material cost, then terminate the design process with the minimum material cost design for the structure; otherwise, return to step 2, update the finite element model using the current set of design variables and repeat the eigenvalue analysis and design optimization process.

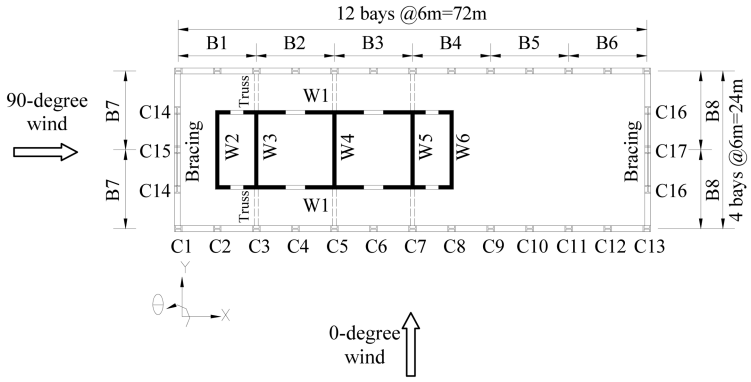

Fig. 1 Structural plan of the 60-story building

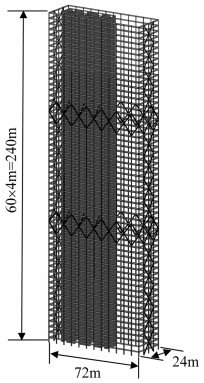

Fig. 2 3D view of the 60-story building

5. Illustrative example

A 60-story office building having a height of 240 m and a rectangular floor plan dimension of 24 m by 72 m is used to illustrate the effectiveness and practical application of the optimal serviceability design technique. As shown in Figs. 1 and 2 the building has adopted basically an outrigger braced system, which consists of a perimeter steel frame connected to an eccentric reinforced concrete core by two levels of 4-story height steel outriggers and belt trusses. Two double-bay X-braced frames are also placed at the two narrow end faces of the building to enhance the torsional rigidity of the building. Since the concrete core is eccentrically located, significant lateral-torsional motion induced by wind loading is anticipated.

The exterior steelwork of the building is to be designed using AISC standard steel sections as follows: W30 shapes for beams; W14 shapes for columns, and diagonals. The eccentric core wall of the building is made of grade C40 concrete. The initial structural element sizes of the building established based on a preliminary strength check are given in Table 2. The first three fundamental frequencies of the finite element model of the initial building are 0.185 Hz (swaying primarily in the short direction of the building), 0.327 Hz (swaying primarily in the long direction) and 0.410 Hz (mainly torsional vibration). The first three associated natural mode shapes of the building are given in Fig. 3.

A wind tunnel test was carried out at the CLP Power Wind/Wave Tunnel Facility (WWTF) of the Hong Kong University of Science and Technology (Tse *et al*. 2007). Wind forces acting on the building were measured by the SMPSS technique using a 1:400 scaled rigid model. The local wind force at each local pressure tap can be calculated as follows

Table 1 Design wind speed at the height of 90 m in Hong Kong area

Design wind speed (m/s)	Return period	Serviceability check
22.5	1 year	Perception threshold (AIJ-GEH)
30.6	5 years	Occupant comfort (ISO-6897)
34.7	10 years	Occupant tolerance (HKCOP)
46.9	50 years	Drift (HKCOP)

Table 2 Initial member sizes for the 60-story building

Concrete core		Exterior steel framework			X brace and truss	
		AISC standard steel section				
Story no.	Wall thickness (mm)	Story no.	Column	Beam	X brace at two end faces	Two levels of outriggers and belt trusses
51-60	300	57-60	W14×34	W30×99	W14×90	
41-50	600	53-56	W14×34	W30×99	W14×90	
31-40	600	49-52	W14×34	W30×99	W14×159	
21+30	800	45-48	W14×159	W30×357	W14×159	
11-20	800	41-44	W14×159	W30×357	W14×159	W14×730
1-10	1000	37-40	W14×257	W30×357	W14×342	
		33-36	W14×257	W30×357	W14×342	
		29-32	W14×370	W30×357	W14×398	
		25-28	W14×370	W30×357	W14×398	
		21-24	W14×370	W30×357	W14×398	
		17-20	W14×500	W30×357	W14×455	
		13-16	W14×500	W30×357	W14×455	
		9-12	W14×730	W30×357	W14×730	W14×730
		5-8	W14×730	W30×357	W14×730	
		1-4	W14×730	W30×357	W14×730	

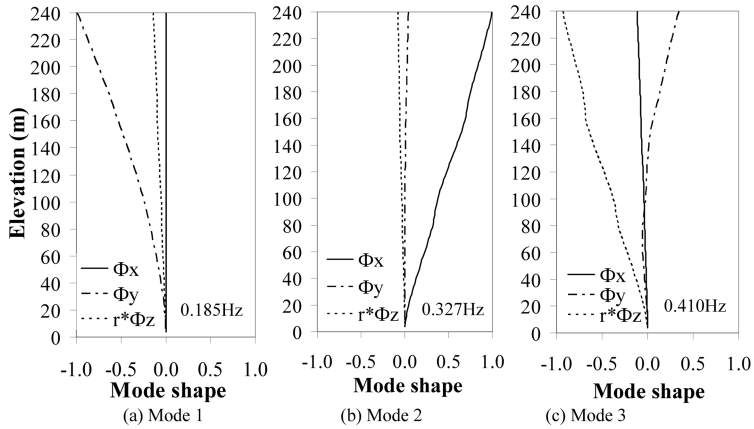

Fig. 3 Coupled 3D mode shapes of the 60-story building

$$F(t) = 0.5\rho\overline{U}^2 C_p(t)\Delta A \tag{44}$$

where ρ is the density of air; $\overline{U}$ is the design hourly mean wind speed; $C_p(t)$ is the pressure coefficient time history at the local position of a pressure tap; ΔA is the tributary area of each pressure tap. Once the collective wind forces of all pressure taps for each floor level were obtained using Eq. (44), the modal wind force time histories were then calculated and the PSD functions of

the modal forces were obtained by Fourier transformation.

According to the acceleration constraints given in Eq. (20) to Eq. (22), 10-year, 5-year and 1-year return periods of wind in a specific urban environment like Hong Kong were considered in evaluating the acceleration performances of the building. Following the Hong Kong Wind Code 2004, the design hourly-mean wind speeds at a reference height of 90 m corresponding to the three different return periods of wind are given in Table 1. Two modal damping ratios for calculating the acceleration and drift responses were assumed to be 1% and 1.5%, respectively. Two specific wind conditions corresponding to two perpendicular incident wind angles were simultaneously considered in the design optimization process. One was the 0-degree wind perpendicular to the wide face acting in the short direction (i.e., along the Y-axis) of the building; another one was the 90-degree wind perpendicular to the narrow face acting in the long direction (i.e., along the X-axis). The PSD functions of the modal forces corresponding to a 10-year return period wind for the building are given in Fig. 4. For the 0-degree wind, the wind-induced modal force spectra within the typical range of frequencies for dynamic serviceability checking (i.e., $0.1\text{Hz} \le f \le 1\text{Hz}$) can be expressed as a function of the modal frequency f as follows

Mode 1: $$S_{Q_{11}} = 4.660 \times 10^{8} f^{-4.069} (\text{N}^2/\text{Hz}) \tag{45}$$

Mode 2: $$S_{Q_{22}} = 2.467 \times 10^{8} f^{-3.808} (\text{N}^2/\text{Hz}) \tag{46}$$

Mode 3: $$S_{Q_{33}} = 3.437 \times 10^{8} f^{-3.835} (\text{N}^2/\text{Hz}) \tag{47}$$

For the incident 90 degree wind, the wind-induced modal force spectra can be written as

Mode 1: $$S_{Q_{11}} = 7.617 \times 10^{8} f^{-3.879} (\text{N}^2/\text{Hz}) \tag{48}$$

Mode 2: $$S_{Q_{22}} = 2.490 \times 10^{8} f^{-3.096} (\text{N}^2/\text{Hz}) \tag{49}$$

Mode 3: $$S_{Q_{33}} = 7.874 \times 10^{8} f^{-4.717} (\text{N}^2/\text{Hz}) \tag{50}$$

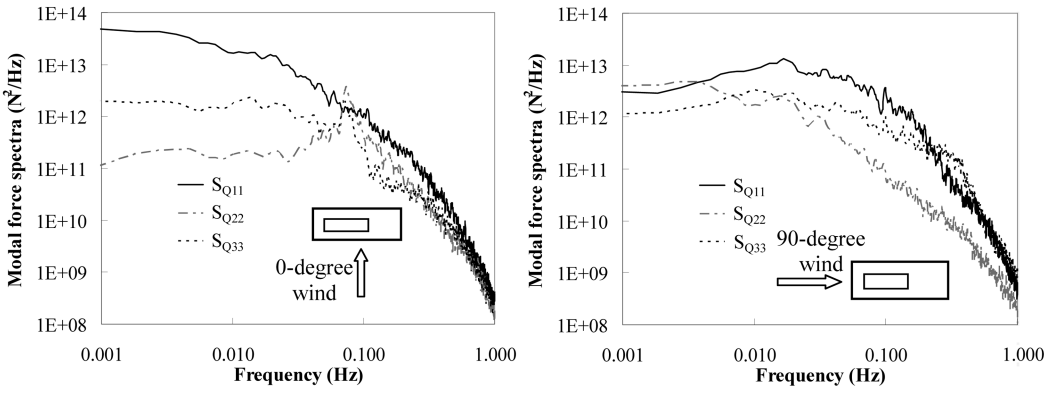

(a) Under the 0-degree wind (b) Under the 90-degree wind

Fig. 4 Power spectral densities of modal forces corresponding to a 10-year return period wind

Table 3 Peak resultant acceleration responses of the 60-story building before optimization

HKCOP (2004) 10-year recurrence wind	Peak resultant acceleration criteria	a_x (milli-g)	a_y (milli-g)	a_θ ×37.95m* (milli-g)	Peak resultant (milli-g)
	0-degree wind	7.9	28.7	15.3	33.5
	90-degree wind	4.9	34.9	27.1	44.3

*The distance 37.95 m is measured from the mass center to the corner position of the building plan.

Table 4 Modal acceleration responses of the 60-story building before optimization

Criteria		Mode 1 (milli-g)	Mode 2 (milli-g)	Mode 3 (milli-g)
ISO-6897 (1984) 5-year recurrence wind	Standard deviation criteria	5.2	4.1	3.8
	0-degree wind	5.6	1.1	1.1
	90-degree wind	6.2	0.8	2.4
AIJ-GEH (2004) 1-year recurrence wind	Peak acceleration criteria	13.1	10.4	9.4
	0-degree wind	6.2	1.3	1.4
	90-degree wind	7.0	1.1	2.5

For other recurrence intervals of wind, the modal force spectra corresponding to a given wind speed V_R in the recurrence interval of R years can be obtained by multiplying Eqs. (48)-(53) associated with the 10-year-recurrence wind speed V_{10} by a factor $(V_R / V_{10})^4$.

The results of the component and resultant acceleration responses of the initial building under 10-year recurrence interval wind are given in Table 3. Due to vortex shedding effects, significant crosswind vibrations in the Y-direction induced by the 90-degree (X-direction) wind is found. For instance, the Y-direction crosswind acceleration component induced by the 90-degree wind on the building is 34.9 milli-g, which is larger than the corresponding Y-direction alongwind acceleration components of 28.7 milli-g under the 0-degree wind. By combining the swaying and torsional acceleration components, the resultant accelerations at the most distant corner of the top floor level of the building are 33.5 milli-g under the 0-degree wind and are 44.3 milli-g under the 90-degree wind as shown in Table 3. Significant violations of 34% and 77% in the peak resultant acceleration criterion of 25 milli-g according to the Hong Kong Codes of Practice (HKCOP 2004, HKCOP 2005) are found for the building under the 0-degree wind and the 90-degree wind, respectively.

For comparison, the habitability or occupant comfort level of the initial building under more frequent 5-year and 1-year return period wind was also assessed based on the frequency dependent ISO-6897 and AIJ-GEH criteria. The modal acceleration responses of the building and the frequency dependent threshold values stipulated in the ISO-6897 and AIJ-GEH are given in Table 4. Before optimization, the building is found to violate the ISO-6897 occupant comfort criteria for the first modal response, but to meet the ISO-6897 criteria for the second and third modes. In terms of standard deviation modal acceleration, the first modal responses of the building violated the ISO-6897 criteria by 8% and 19% under the 0-degree wind and the 90-degree wind, respectively. In terms of peak modal accelerations, the initial building structure is found to meet the AIJ-GEH criteria for all three modes under both the 0-degree and 90-degree wind conditions.

For this 60-story building with 3D coupled modes, the frequency independent peak resultant acceleration criteria appear to be most stringent, while the ISO-6897 frequency dependent standard

deviation modal acceleration criteria based on 5-year return period wind seem to be stricter than the AIJ-GEH peak modal acceleration criteria based on 1-year return period wind. Since the peak resultant acceleration response captures not only the mechanically coupled swaying and torsional effects but also the modal combination effects including torsional amplification at the corner positions, designing the building to satisfy the resultant acceleration criteria is thus more challenging than that the modal acceleration criteria of the ISO-6897 or AIJ-GEH. One of the reasons for the seemingly more constraining peak resultant criterion is that the modal criteria have been divided and assessed by the modal values without considering the multi-dimensional response. The other reason is the different recurrence intervals used in the various criteria. Since the evaluation of N-year-recurrence wind speed is a result of wind climate, it can be reasoned that the initial building satisfying the AIJ-GEH one year acceleration criteria but not the ten-year HKCOP may be a direct result of the typhoon-dominated Hong Kong wind climate. In other regions dominated by synoptic winds, the AIJ-GEH and ISO6897 criteria may become more onerous than other ten-year return period peak resultant criteria.

In order to study the influence of the occupant comfort criteria on the optimal stiffness design of the building, four optimization cases with different consideration of drift and acceleration constraints are considered:

Case 1: consideration of drift constraints only.

Case 2: drift constraints and the ISO-6897 standard deviation modal acceleration constraints.

Case 3: drift constraints and the AIJ-GEH peak modal acceleration constraints.

Case 4: drift constraints and the HKCOP peak resultant acceleration constraints.

Fig. 5 presents the material cost design histories of the building for all four cases. The normalized cost with respect to the initial structural material cost of the building is given for each design cycle, which includes the process of one formal response analysis and one resizing optimization. Although the structural cost of the building was found somewhat fluctuating for the first few design cycles, steady convergence to the final optimum solution was achieved for all 4 cases. Cases 1, 2 and 3 have converged to almost the same value of the normalized cost (i.e., 0.962 for case 1, 0.971 for case 2 and 0.958 for case 3). Such a result and a subsequent check on the final element sizes of the optimized structures indicate that the standard deviation modal acceleration constraints in case 2 and the peak modal acceleration constraints in case 3 have relatively little influence on the optimized

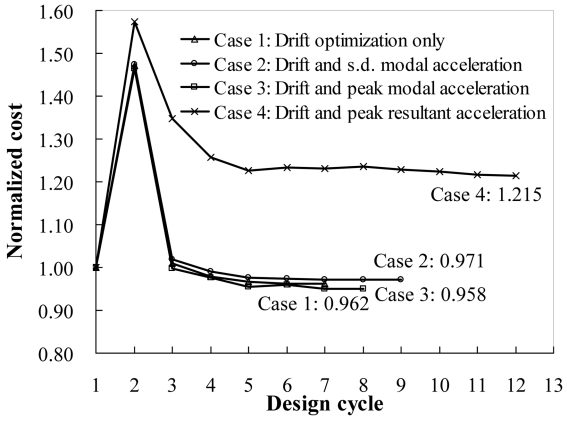

Fig. 5 Design histories of the normalized structure cost of the 60-story building

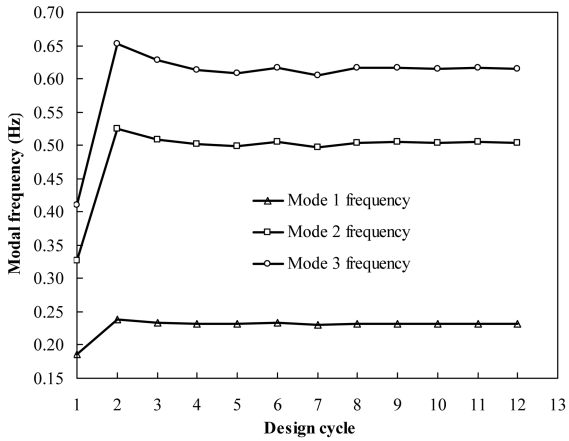

Fig. 6 Design histories of modal frequencies of the 60-story building for case 4

building structure. It is evident that the optimized designs of the first three cases are mainly governed by the static drift constraints rather than by the dynamic modal acceleration constraints. When both static drift and peak resultant acceleration constraints are considered in case 4, an increase of about 21.5% in the material cost is needed to fulfill both the drift and peak resultant acceleration constraints, indicating that the peak resultant acceleration has greatly influenced on the final design of the structure.

Tables 5 and 6 present the acceleration responses of the optimized building and the evaluation of habitability after optimization. As shown in Table 5, the modal acceleration responses of the optimized structure are found to be within the ISO-6897 standard deviation modal acceleration limit for case 2, and within the AIJ-GEH peak modal acceleration limit for case 3. In case 4, the initial peak resultant response of 44.3 milli-g is greatly reduced by 56% to slightly below the limiting

Table 5 Modal acceleration responses of the 60-story building after optimization

Criteria		Mode 1 (milli-g)	Mode 2 (milli-g)	Mode 3 (milli-g)
ISO-6897 (1984) 5-year recurrence wind	Standard deviation criteria	4.8	3.6	3.3
	0-degree wind	4.1	0.7	0.7
	90-degree wind	4.6	0.5	1.3
AIJ-GEH (2004) 1-year recurrence wind	Peak acceleration criteria	12.0	8.6	7.9
	0-degree wind	4.6	0.8	0.9
	90-degree wind	5.3	0.7	1.4

Table 6 Peak resultant acceleration responses of the 60-story building after optimization

HKCOP(2004) 10-year recurrence wind	Peak resultant acceleration criteria	a_x (milli-g)	a_y (milli-g)	$a_\theta \times 37.95$ m (milli-g)	Peak resultant (milli-g)
	0-degree wind	3.9	21.6	6.1	22.8
	90-degree wind	2.7	23.2	8.9	24.9

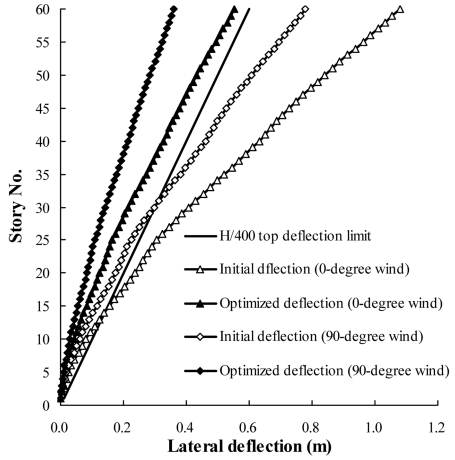

Fig. 7 Lateral deflection profiles of the 60-story building for case 4

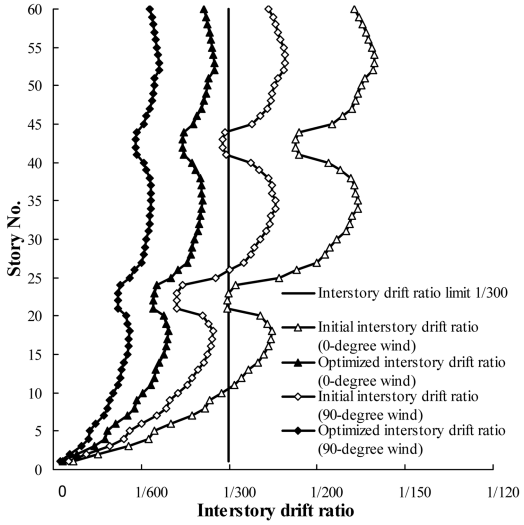

Fig. 8 Interstory drift ratio profiles of the 60-story building for case 4

value of 25 milli-g. The component and resultant acceleration responses at the top corner of the building after optimization are given in Table 6. It is found that all three acceleration components have been reduced by the stiffness design optimization technique. The most significant reduction of acceleration is the acceleration component caused by the torsional effect. For example, the torsional acceleration components at the top corner of the building are reduced by 60.1% (from 15.3 to 6.1 milli-g) and 67.1% (from 27.1 to 8.9 milli-g) under the 0-degree wind and the 90-degree wind, respectively. It is believed that the large reduction in the torsional acceleration is due to the significant improvement in the torsional rigidity of the building by the computer based optimization technique.

Fig. 6 presents the modal frequency histories for case 4. Similar to the cost history of case 4, a steady convergence to the optimum frequency values has also been achieved with a noticeable

fluctuation for the first few design cycles. Figs. 7 and 8 present the initial and final lateral deflections profiles and interstory drift ratio profiles at the most critical corner column of the building for case 4. It is clearly shown that the initial design established solely based on strength check are found to violate considerably in both the top deflection limit (i.e., H/400, where H = building height) and interstory drift ratio limit (i.e., 1/300). With a wider frontal face in the 0-degree wind, much larger lateral deflection and interstory drift responses in the short direction (i.e., along the Y-axis) of the building are found as shown in Figs. 7 and 8. After the optimization, no violation in both the top deflection and the interstory drift responses are found for the optimized building under the 0-degree wind and the 90-degree wind. It is noted that the two kinks on each interstory drift ratio profile as shown in Fig. 8 indicate the two levels of the steel outriggers and belt trusses.

6. Conclusions

This paper presents an integrated wind-induced dynamic analysis and automatic computer-based design optimization technique for minimizing the structural cost of tall buildings subject to static and dynamic serviceability design criteria. Using wind tunnel derived aerodynamic wind load spectra, the coupled dynamic response of a tall building under spatiotemporally varying wind excitation is analyzed based on random vibration theory. The optimal design problem of general tall building structures subject to both the static drift constraints and the dynamic occupant comfort acceleration constraints have been explicitly expressed in terms of element sizing design variables. A rigorously derived Optimality Criteria (OC) method has been developed for solving the optimal stiffness design problem. Results of a full-scale 60-story hybrid building with 3D mode shapes have shown that the stiffness design optimization technique provides a powerful design tool for the static drift and dynamic occupant comfort serviceability design of tall buildings. Not only is the computer-based optimization technique capable of achieving the most economical distribution of element stiffness of practical tall building structures while satisfying multiple static drift and dynamic acceleration serviceability design requirements, but also the numerical optimal design method is computationally efficient since the final optimal design can generally be obtained in only a few number of reanalysis and redesign cycles. Both frequency independent peak resultant acceleration criteria and frequency dependent standard deviation or peak modal acceleration criteria have been considered in the optimization process due to their different implication in the evaluation of habitability. It is noteworthy that the stiffness design optimization works well for typical tall buildings but may not be effective for all tall buildings. Furthermore, in some special cases the peak resonant dynamic response is insensitive to changes in modal frequencies, and hence other mitigating measures may become necessary.

Acknowledgements

The work described in this paper was partially supported by the Research Grants Council of the Hong Kong Special Administrative Region (Project No. CA04/05.EG01) and the National Natural Science Foundation of China (Project Nos. 51008275, 90815023 and 51021140006).

References

Architectural Institute of Japan Recommendations (2004), *Guidelines for the evaluation of habitability to building vibration*, AIJ-GEH-2004, Tokyo, Japan.

Banavalkar, P.V. (1990), "Structural systems to improve wind induced dynamic performance", *J. Wind Eng. Ind. Aerod.*, **36**, 213–224.

Boggs, D. (1995), *Acceleration indexes for human comfort in tall buildings-peak or RMS?*, CTBUH Monograph Chapter 13, Council on Tall Buildings and Urban Habitat.

Burton, M.D., Kwok, K.C.S., Hitchcock, P.A. and Roy, O.D. (2006), "Frequency dependence of human response to wind-induced building motion", *J. Struct. Eng*., **132**(2), 296-303.

Burton, M.D., Kwok, K.C.S. and Hitchcock, P.A. (2007), "Occupant comfort criteria for wind-excited buildings: based on motion duration", *Proc. 12th International Conference on Wind Engineering*, Cairns, Australia, 2 – 6 July, 2007, 1207-1214.

Cermak, J.E. (2003), "Wind-tunnel development and trends in applications to civil engineering", *J. Wind Eng. Ind. Aerod.*, **91**, 355–370.

Chan, C.M. (2001), "Optimal lateral stiffness design of tall buildings of mixed steel and concrete construction", *J. Struct. Des. Tall Build*., **10**(3), 155-177.

Chan, C.M. (2004), "Advances in structural optimization of tall buildings in Hong Kong", *Proc. 3rd China-Japan-Korea Joint Symposium on Optimization of Structural and Mechanical Systems*, Kanazawa, Japan, 30 Oct. – 2 Nov., 2004, 49-57.

Chan, C.M. and Chui, J.K.L. (2006),"Wind-induced response and serviceability design optimization of tall steel buildings", *J. Eng. Struct*., **28**(4), 503-513.

Chan, C.M., Chui, J.K.L. and Huang, M.F. (2009), "Integrated aerodynamic load determination and stiffness optimization of tall buildings", *J. Struct. Des. Tall Spec. Build*., **18**, 59–80.

Chang, F.K. (1967), "Wind and movement in tall buildings", *Civil Eng*., **37**(8), 70-72.

Chang, F.K. (1973), "Human response to motions in tall buildings", *J. Struct. Division*, **99**(6), 1259-1272.

Chen, P.W. and Robertson, L.E. (1973), "Human perception threshold of horizontal motion", *J. Struct. Division*, **8**(8), 1681-1695.

Chen, X. and Kareem, A. (2005a), "Coupled dynamic analysis and equivalent static wind loads on buildings with three-dimensional modes", *J. Struct. Eng*., **131**(7), 1071-1082.

Chen, X. and Kareem, A. (2005b), "Dynamic wind effects on buildings with 3D coupled modes: application of high frequency force balance measurements", *J. Eng. Mech*., **131**(11), 1115-1125.

Davenport, A.G. (1964), "Note on the distribution of the largest value of a random function with application to gust loading", *Proc. Inst. Civil Eng*., **28**, 187-196.

Goto, T., Iwasa, Y. and Tsurumaki, H. (1990), "An experimental study on the relationship between motion and habitability in a tall residential building", *Proceedings of Tall Buildings: 2000 and Beyond, Fourth World Congress*, Hong Kong, 817-829.

Griffis, L.G. (1993), "Serviceability limit states under wind load", *Eng. J. AISC*, **30**(1), 1-16.

Hansen, R.J., Reed, J.W. and Vanmarcke, E.H. (1973), "Human response to wind-induced motion of buildings", *J. Struct. Division*, **99**(ST7), 1589-1605.

Hong Kong Code of Practice (2004), *Code of practice for structural use of concrete*, Buildings Department, Hong Kong.

Hong Kong Code of Practice (2005), *Code of practice for structural use of steel*, Buildings Department, Hong Kong.

Huang, M.F. and Chan, C.M. (2007), "Sensitivity analysis of multi-story steel building frameworks under wind and earthquake loading", *Proc. 7th World Congresses of Structural and Multidisciplinary Optimization*, COEX Seoul, Korea, 21 – 25 May, 2007, 1376-1385.

Huang, M.F., Chan, C.M., Kwok, K.C.S. and Hitchcock, P.A. (2009), "Cross correlation of modal responses of tall buildings in wind-induced lateral-torsional motion", *J. Eng. Mech. - ASCE*, **135**(8), 802-812.

International Organization for Standardization (1984), *Guidelines for the evaluation of the response of occupants of fixed structures, especially buildings and offshore structures, to low-frequency horizontal motion (0.063 to 1.0 Hz) ISO 6897:1984*, International Organization for Standardization, Geneva, Switzerland.

International Organization for Standardization (2007), *Serviceability of buildings and walkways against vibrations: Annex D, ISO 10137:2007*, International Organization for Standardization, Geneva, Switzerland.
Irwin, A.W. (1978), "Human response to dynamic motion of structures", *Struct. Eng*., **56**(9), 237-243.
Islam, S., Ellingwood, B. and Corotis, R.B. (1992), "Wind-induced response of structurally asymmetric highrise buildings", *J. Struct. Eng*., **118**(1), 207-222.
Isyumov, N. (1982), "The aeroelastic modeling of tall buildings", *Wind Tunnel Modeling for Civil Engineering Applications*, T. A. Reinhold (ed.), 373-407.
Isyumov, N., Fediw, A.A., Colaco, J. and Banavalkar, P.V. (1992), "Performance of a tall building under wind action", *J. Wind Eng. Ind. Aerod.*, **41-44**, 1053-1064.
Isyumov, N., Mascantonio, A. and Davenport, A.G. (1988), "Measured building motions of tall buildings in wind and their evaluation", *Symposium/Workshop on Serviceability of Buildings (Movements, Deformations, Vibrations)*, Ottawa, Canada, 16-18 May.
Isyumov, N. and Kilpatrick, J. (1996), "Full-scale experience with wind-induced motions of tall buildings", *Proceedings of the 67th Regional Conference Council on Tall Buildings and Urban Habitat*, Chicago, US, 15-18 April, 401-411.
Kareem, A. (1985), "Lateral-torsional motion of tall buildings to wind loads", *J. Struct. Eng*., **111**(11), 2479-2496.
Kareem, A. (1992), "Dynamic response of high-rise buildings to stochastic wind loads", *J. Wind Eng. Ind. Aerod.*, **41-44**, 1101-1112.
Kwok, K.C.S., Burton, M.D. and Hitchcock, P.A. (2007), "Occupant comfort and perception of motion in wind-excited tall buildings", *Proc. 12th International Conference on Wind Engineering*, Cairns, Australia, 2 – 6 July, 2007, 101-115.
Kwok, K.C.S., Hitchcock, P.A. and Burton, M.D. (2009), "Perception of vibration and occupant comfort in wind-excited tall buildings", *J. Wind Eng. Ind. Aerod.*, **97**, 368-380.
Lee, B.E. (1983), "The perception of the wind-induced vibration of a tall building-a personal viewpoint", *J. Wind Eng. Ind. Aerod.*, **12**, 379-384.
Melbourne, W.H. and Palmer, T.R. (1992), "Accelerations and comfort criteria for buildings undergong complex motions", *J. Wind Eng. Ind. Aerod.*, **41-44**, 105-116.
National Building Code of Canada (1977), *Structural commentaries (Part 4)*, National Research Council of Canada, Ottawa, Ontario.
National Building Code of Canada (1995), *Structural commentaries (Part 4)*, National Research Council of Canada, Ottawa, Ontario.
National Standard of the People's Republic of China (2002), *Technical specification for concrete structures of tall building (JGJ 3-2002)*, New World Press, Beijing, China.
Tallin, A. and Ellingwood, B. (1985), "Wind induced lateral-torsional motion of buildings", *J. Struct. Eng*., **111**(10), 2197-2213.
Tamura, Y., Kawana, S., Nakamura, J., Kanda, J. and Nakata, S. (2006), "Evaluation perception of wind-induced vibration in buildings", *Proceedings of the Institution of Civil Engineers: Structures & Buildings*, **159**, 283-293.
Tse, T., Kwok, K.C.S., Hitchcock, P.A., Samali, B. and Huang, M.F. (2007), "Vibration control of a windexcited benchmark tall building with complex lateral-torsional modes of vibration", *Adv. Struct. Eng*., **10** (3), 283-304.
Vickery, B.J., Isyumov, N. and Davenport, A.G. (1983), "The role of damping, mass and stiffness in the reduction of wind effects on structures", *J. Wind Eng. Ind. Aerod.*, **11**, 285–294.
Yip, D.Y.N. and Flay, R.G.J. (1995), "A new force balance data analysis method for wind response predictions of tall buildings", *J. Wind Eng. Ind. Aerod.*, **54-55**, 457-471.